UDK 519.61/.64:669.58:669.14.018.291
Original scientific article/Izvirni znanstveni članek

ISSN 1580-2949
MTAEC9, 47(2)161(2013)

DISTORTION OF THE SUBSTRUCTURE OF A 20-ft SHIPPING CONTAINER EXPOSED TO ZINC HOT-DIP GALVANIZING

SPREMINJANJE MER PODSTRUKTURE PRI 20 ft TRANSPORTNEM KONTEJNERJU PRI VROČEM POTOPNEM CINKANJU

Ivana Ivanović[1], Aleksandar Sedmak[2], Rebeka Rudolf[3], Leo Gusel[3], Biljana Grujić[1]

[1]Innovation Center, Faculty of Mechanical Engineering, University of Belgrade, Kraljice Marije 16, 11000 Belgrade, Republic of Serbia
[2]Faculty of Mechanical Engineering, University of Belgrade, Kraljice Marije 16, 11000 Belgrade, Republic of Serbia
[3]University of Maribor, Faculty of Mechanical Engineering, Smetanova ulica 17, 2000 Maribor, Slovenia
iivanovic@mas.bg.ac.rs

Prejem rokopisa – received: 2012-08-21; sprejem za objavo – accepted for publication: 2012-10-03

The main goal of this study was to build a model for a numerical simulation of hot-dip galvanizing of a 20-ft ISO shipping container. For that purpose, the basic transient thermo-mechanical problem of a steel structure under the influence of the temperature characteristic for a zinc hot-dip galvanizing bath was analyzed. Numerical calculations were performed for a simple part and for the complex substructure of the container. Calculations were carried out on the Salome-Meca platform using a Netgen mesh generator and a Code_Aster finite-element solver.

Keywords: shipping container, structural steel, zinc hot-dip galvanizing, transient heat transfer, distortion

Glavni namen te študije je bila izdelava modela za numerično simulacijo vročega potopnega cinkanja 20 ft ISO transportnega kontejnerja. Zato smo analizirali osnovni termomehanski problem jeklene konstrukcije zaradi vpliva toplote med vročim potopnim cinkanjem. Numerični izračuni so bili izvršeni za enostavni del in za kompleksno podstrukturo kontejnerja. Izračuni so bili izvršeni na platformi Salome-Meca z uporabo generatorja mreže Netgen in programske opreme Code_Aster na osnovi metode končnih elementov.

Ključne besede: transportni kontejner, konstrukcijsko jeklo, vroče potopno cinkanje, prenos toplote, deformacija konstrukcije

1 INTRODUCTION

This study is a part of a wider research launched in order to develop an innovative 20-ft ISO shipping container with a longer lifetime. Since shipping containers have to face hard handling and hard weather conditions, zinc hot-dip galvanizing, if possible, in the form of an integrated welded structure, may represent the best way to achieve this goal.

The dimensions of the 20-ft ISO shipping container are 6.058 m × 2.348 m × 2.591 m with a net weight of approximately 2 400 kg. The skeleton of the container is composed of various steel profiles made of 235–420 graded structural steel. Profiles are welded to the cubical corner fittings thus forming an orthogonal skeleton. The wall and roof panels are composed of welded corrugated steel sheets. The panels are welded continually to the rest of the structure. The material thickness varies depending upon the type of the element.

The entire skeleton will be taken into consideration as a numerical model, despite the fact that the 20-ft shipping container is larger than any existing galvanizing bath, which means that in actual conditions it cannot be galvanized as a whole.[1] On the other hand, it seems that it would be much more efficient to complete most of the construction before galvanizing. Welding of galvanized steel is possible, but it requires a special approach that differs greatly from the standard steel welding techniques.[2]

The temperature of the zinc bath is slightly above 450 °C. If other requirements for the preparation of an object for galvanizing are fulfilled, this temperature should not have a great influence on the mechanical properties of the structural steel in the mentioned structural steel grades.[1,3] Problems were expected to arise due to an extremely complex structure. For example, one of the most important requirements for galvanizing is that the thickness of the material of different parts that are going to be galvanized together must be as uniform as possible. Large differences in the thicknesses will result in different heating and cooling of the material, and will increase the risk of undesirable large distortions. In the case of the shipping container, the thickness ranges from 28 mm in some regions of the corner fittings, 4.5 mm to 12 mm for the profiles in the skeleton and, finally, to 2 mm for the wall panel.

Problems will also arise in several areas of the structure where the hollow sections are completely sealed by the other parts of the structure. These sections must be replaced with open sections or vent/drain holes must be provided. An even greater problem is the

numerous corners of the element connections that also need to be supplied with vent/drain holes.

When it comes to numerical simulation, there is very little information on previous studies dealing with zinc hot-dip galvanizing, especially those dealing with the fluid dynamics of zinc at the temperature of the galvanizing bath, and the fluid dynamics of the galvanizing bath. Some insight into the field could be gained from a thermal analysis carried out, during the solidification, on the moving surface in a finite bath given in [4]. Concerning a transient three-dimensional thermo-mechanical numerical analysis, there is a great number of papers dealing with this subject within the welding researches.[5–8] The basic thermo-mechanical analysis, at some level similar to this one, is performed and described in [9,10].

This is a highly idealized analysis of a real-time problem, and numerous real-time conditions are ignored deliberately.

2 GENERAL-MODELING DESCRIPTION

2.1 Geometry of the model

The skeleton used as a model for numerical simulations of the zinc hot-dip galvanizing of a 20-ft ISO shipping container is presented in **Figure 1**. The skeleton model is composed of two front-corner posts, two outer rear-corner posts, two bottom side rails, two top side rails, a door sill, the lower part of the door header, a front sill, a front-top end rail, three types of floor cross-members, two forklift-pocket top plates and, finally, four top- and four bottom-corner fittings.

It was already mentioned that some elements in the construction should be omitted or replaced in order to avoid closed hollow sections. Such sections are undesirable in galvanizing, but also need special treatment during a numerical simulation. The initial examples, the most sensitive to changes, are the corner posts. The

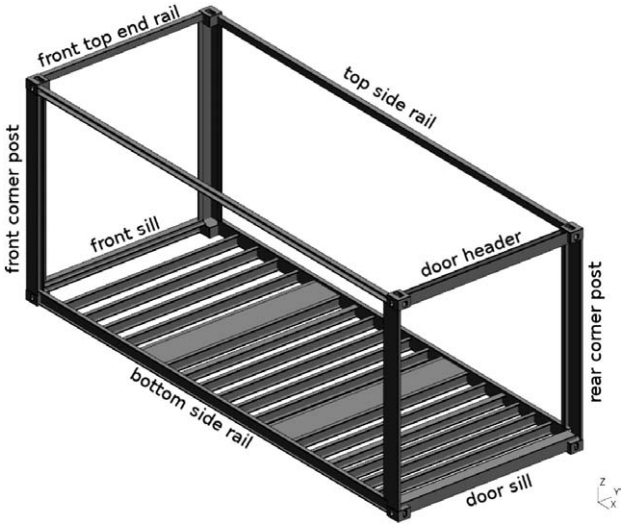

Figure 1: Skeleton of the 20-ft ISO shipping container
Slika 1: Ogrodje 20 ft ISO ladijskega kontejnerja

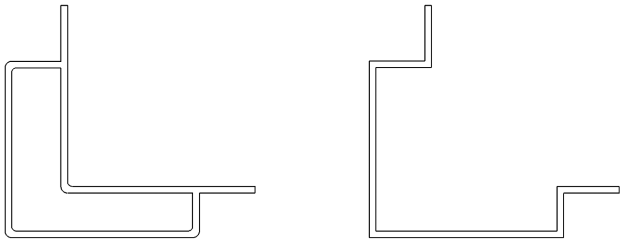

Figure 2: Cross sections of the front-corner-post profiles
Slika 2: Prereza profilov kotnih drogov v sprednjem delu

front-corner post is planned to be a 6 mm thick, S235JR-steel closed profile as illustrated in **Figure 2** (left). When welded to the corner fittings, this profile will form a closed hollow section. Therefore, in simulations, the closed profile is replaced by a standard-shaped open profile of the same thickness as illustrated in **Figure 2** (right). To simplify an already complex geometry, the edge filleting is omitted here, as well as for all the other elements.

The rear-corner-post profile consists of an inner and outer part. A standard 6 mm thick outer profile, planned to be made of the S420NL steel, is kept in the numerical model. The inner part could not be omitted from the real skeleton, but it is assumed that it can be added afterwards. The notches for door-hinge-pin lugs, which are usually made on the outer part of the rear-corner post, are omitted to simplify the geometry.

Bottom side rails (4.5 mm S420NL steel) are introduced without the two forklift-pocket openings. Only the standard U-shaped lower part of the door header (4 mm S355NL steel) is included. For the two top side rails and for the front-top end rail (4 mm S355NL steel), the standard square tubes are replaced with the channel-shaped steel sections.

The elements of the skeleton are connected to the construction with corner fittings. The dimensions of the corner fittings are much smaller than the dimensions of the other elements, 178 mm × 162 mm × 118 mm, but the thickness of the walls is much higher, and it ranges from 10 mm to 28 mm. They have a specific geometry since they are designed for lifting, stacking and securing the container. The real form of the top-corner fitting is illustrated in **Figure 3** (left). A simplified form, attached

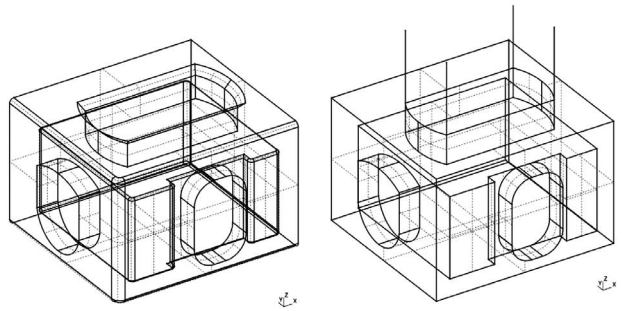

Figure 3: Top-corner-fitting geometry
Slika 3: Geometrija gornjega vogala

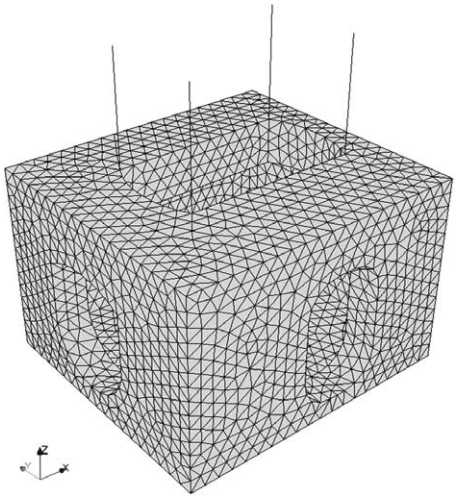

Figure 4: Example of a Netgen three-dimensional tetrahedral mesh
Slika 4: Primer tridimenzionalne tetraedrične mreže Netgen

to the cables in a way that will be used for numerical simulations, is presented in **Figure 3** (right).

2.2 Numerical procedures

All pre-processing and post-processing work is performed using an open-source Salome-Meca platform. From the mesh module in Salome-Meca, an open-source Netgen mesh generator is applied to generate an automatic three-dimensional tetrahedral mesh. An example of the mesh generated on the top-corner fitting, with the maximum edge size of 9 mm, resulting in 14 358 tetrahedral elements, is illustrated in **Figure 4**.

The molten zinc bath is kept at a constant temperature of 450 °C during all numerical simulations. The top-corner fitting and the whole skeleton are chosen separately for the simulations. The bottom side of each model is placed in an xy plane. The plane is placed so as to be parallel to the surface of the zinc bath. The models are suspended with four steel cables (**Figure 3** (left) and **Figure 4**). In this manner, for the purpose of the numerical model of the skeleton, the mechanism for vertical lifting of the container from the top corner fittings is simplified and replaced only by cables. Cable thickness is selected so that its elongation is reduced to a minimum.

A transient thermomechanical analysis is performed with the open-source finite-element solver Code_Aster. The thermomechanical properties of the steel are kept constant during the simulations. In the linear thermal analysis, convection boundary conditions are imposed on all the surfaces. An immersion is simulated at a constant velocity of 0.004 m/s and with two different constant heat-transfer coefficients, one at the immersed surfaces and the other at the surfaces outside the zinc bath. The initial temperature of the object and the temperature of the surroundings are the same, 25 °C. The thermal loads and the weight of the model are introduced in a non-linear static analysis. The cables are fixed at one end and connected to the selected points of the object (the corner fitting or skeleton) at the other end.

3 RESULTS AND DISCUSSIONS

Simulations were performed on a desktop PC with an Intel Core i5-2300 CPU running at 2.8 GHz and with 4 GB RAM. Because of the limited computer resources, a simple top-corner fitting model was chosen for general model verifications and validations.

3.1 Top-corner fitting

Corner fittings are the smallest parts of a container construction with very different wall thicknesses. Points 8, 9, 10 and 11, which were used for the presentations of the results obtained for different mesh densities, are illustrated in **Figure 5**. The thickness of the walls around the bottom point 9 is 20 mm on the sides and 10 mm at the bottom. The thickness around the bottom point 8 is 20 mm and 10 mm on the sides. The thickness of the top wall, where points 11 and 10 are situated, is approximately 28 mm. In the case of a velocity of 0.004 m/s, the corner fitting is fully immersed after approximately 30 s.

The temperature results for the selected points are illustrated in **Figure 6a**. The results are presented from the beginning of the simulation until 630 s. It can be seen that the temperatures of four points differ throughout the entire simulation. The maximum value of the temperature difference between the two bottom points is approximately 33 °C, and is reached at 240 s. The temperature of the zinc bath was not reached at the end of the simulation, despite the fact that the corner fitting was immersed fully for 10 min. The maximum temperature was reached at point 8 and has the value of 408 °C.

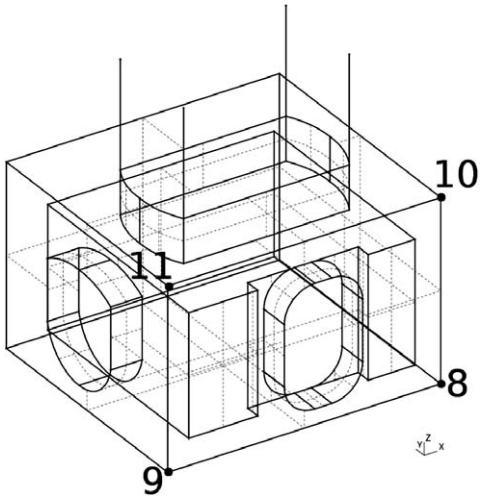

Figure 5: Positions of points 8, 9, 10 and 11
Slika 5: Pozicije točk 8, 9, 10 in 11

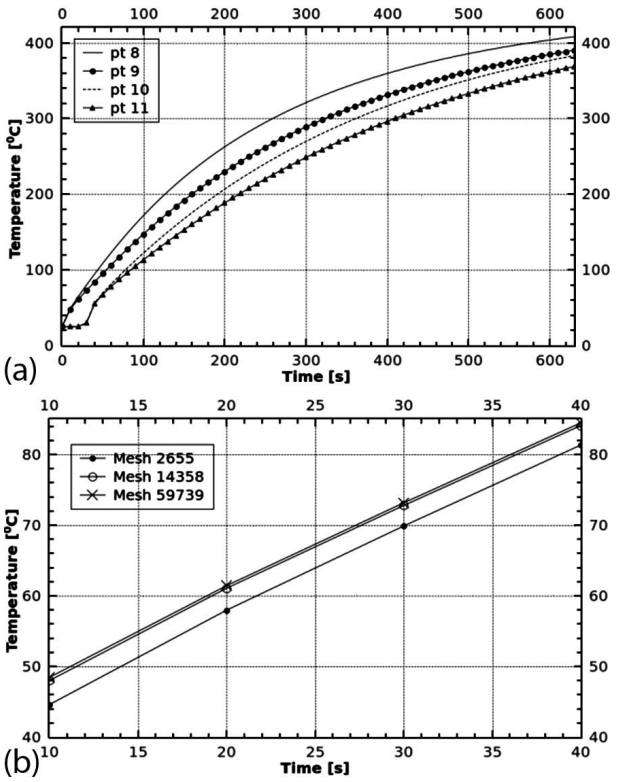

Figure 6: a) Temperature at points 8, 9, 10 and 11 from the beginning of the simulation until 630 s for the mesh of 14 358 elements and b) the temperature at point 9 for three different mesh densities from 10 s to 40 s

Slika 6: a) Temperature v točkah 8, 9, 10 in 11 od začetka simulacije do 630. sekunde za mrežo s 14 358 elementi in b) temperature v točki 9 za tri gostote mreže od 10. sekunde do 40. sekunde

The results obtained using three different mesh densities are presented in **Figure 6b**. The values for the coarse mesh of 2 655 elements (the maximum edge size is 20 mm) are significantly different from the other two sets of values (for the mesh of 14 358 elements the maximum edge size is 9 mm, and for the mesh of 59 739 elements the maximum edge size is 5 mm). The difference was around 3.5 °C at the beginning of the simulation, and around 1 °C at the end of the simulation.

At the beginning of the simulation the temperature at some points of the mesh fell below the assigned initial temperature of the model, which is equal to the temperature of the surroundings. This error decreased with an increase in the mesh density.

The previous discussions are confirmed with **Figure 7**, where the temperature distribution, at 30 s (**a**) and at 630 s (**b**), is presented for the mesh of 14 358 elements. At 30 s, when the phase of immersion is just finished, some parts of the corner fitting are still at the initial temperature of 25 °C. This is an obvious consequence of the already mentioned numerical error caused by the finesse of discretization.

Compared to the temperature of the other previously selected points (**Figure 5**), the highest temperature is in the vicinity of point 8, and is around 80 °C. The tempe-

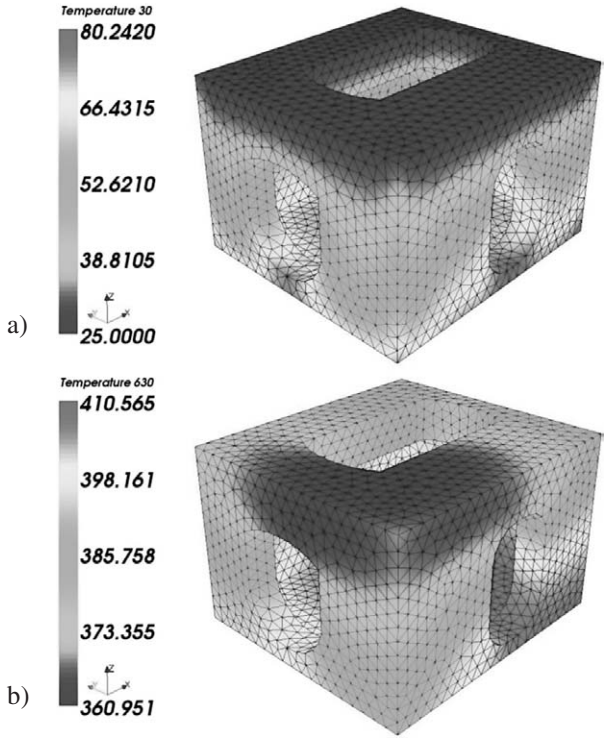

Figure 7: Temperature distribution at the top-corner fitting at: a) 30 s and b) at 630 s for the mesh of 14 358 elements

Slika 7: Razporeditev temperature v vrhnjem kotnem spoju pri: a) 30 s in b) pri 630 s za mrežo s 14 358 elementi

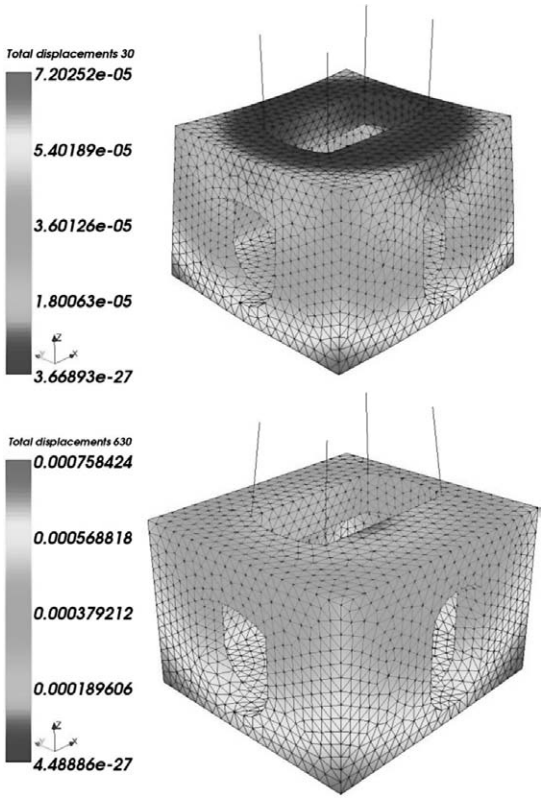

Figure 8: Total displacements at the top-corner fitting at 30 s (scale 200) and at 630 s (scale 40) for the mesh of 14 358 elements

Slika 8: Skupni raztezki v vrhnjem kotnem spoju pri 30 s (skala 200) in pri 630 s (skala 40) za mrežo s 14 358 elementi

rature difference between these points is even more evident at the end of the simulation as illustrated in **Figure 7b**. At 630 s, the maximum temperature is approximately 410 °C, and it is 40 °C lower than the temperature of the zinc bath. The corresponding total displacements are illustrated in **Figure 8**.

3.2 Skeleton

In the case of the skeleton, two mesh densities were used for numerical simulations. The maximum edge size of the finer mesh was equal to the critical edge size of the corner fitting (20 mm). The immersion phase takes approximately 648 s. Because of the limited computer resources, a coarser mesh of 241 623 elements (the maximum edge size of 60 mm) was used to reach the end of the immersion phase. The total displacements and temperature distributions at (50, 350, and 650) s are illustrated in **Figure 9**.

As expected, for this mesh density the minimum temperature at any time was lower than the initial temperature of 25 °C. The temperature of the zinc bath was almost reached at the lower parts of the skeleton by the end of the simulation. The maximum temperature at 650 s, illustrated in **Figure 9** (bottom right), was approximately 449 °C.

It is not hard to notice large differences in the temperature at different positions of the skeleton. Especially at the beginning of the immersion, these temperature differences can produce large distortions. For example, from the temperature distribution at 50 s illustrated in **Figure 9** (top right), it can be seen that the temperature is much higher at the bottom than at the top of the bottom side rails. The temperature of the bottom-corner fittings is even lower. The largest distortions are found in the central area of the floor construction, at the central cross members, and at the two forklift-pocket top plates (**Figure 9** (top left)). There is an obvious distortion of the bottom side rails. This distortion affects the very end of the front corner posts, near the corner fittings. The influence of the distortion of the floor construction on the outer part of the rear corner posts is even more pronounced, but it is also better distributed along the posts than in the case of the front corner posts. At 350 s, the top side rails started to deform as a result of the distortion of the lower half of the skeleton (**Figure 9** (center right)).

The maximum value of the total displacements reached in the first 50 s is around 12.5 mm, in the next 300 s it is increased by only 5 mm, and in the next 300 s it is increased by an even smaller value of only 3 mm.

The influence of the mesh density, for the mesh of 241 623 elements with the maximum edge size of 60 mm, and the mesh of 490 420 elements with the maximum edge size of 20 mm, from 80 s to 120 s, at the point 621 with the coordinates (0, 0, 0), is illustrated in **Figure 10**. A simulation for the finer mesh was executed for the period of up to 200 s. The temperature difference was between 3.5 °C at the beginning of the simulation and 2.5 °C at 200 s. The values of the total displacements, from 80 s to 120 s, were higher for the coarser mesh.

The temperature at different points on the bottom-corner fitting and in its vicinity is presented in **Figure 11**. During the simulation, the temperature was the highest at point 4 067, which is at the bottom of the front sill, and at point 31 870, which is at the bottom of the bottom side rail. The thickness of the material of these profiles is 4.5 mm.

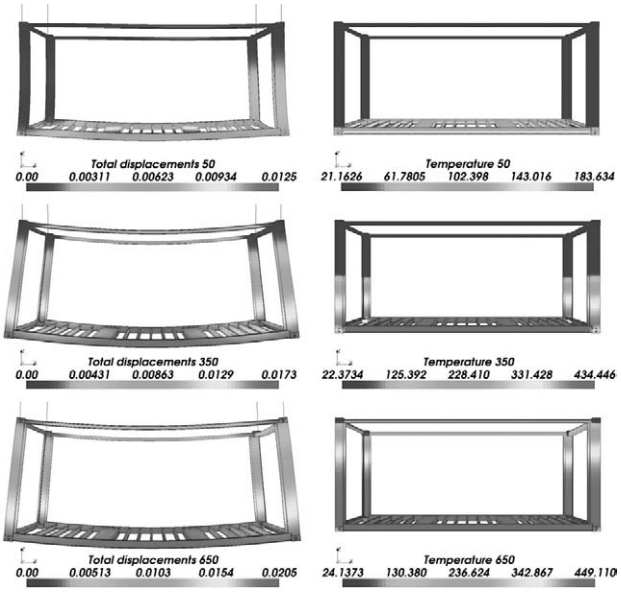

Figure 9: Total displacements (the scale factor of 20) and temperature distributions at (50, 350, and 650) s for the skeleton in the case of a mesh of 241 623 elements (the maximum edge size of 60 mm)

Slika 9: Celotni raztezek (faktor skale 20) in razporeditev temperature pri (50, 350 in 650) s za ogrodje v primeru mreže z 241 623 elementi (maksimalna velikost roba 60 mm)

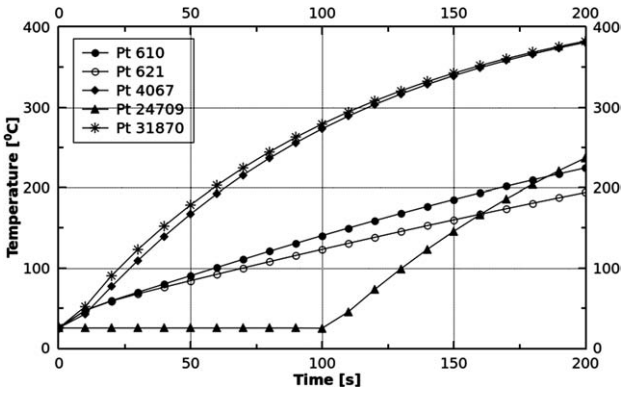

Figure 10: Temperature and total displacements at point (0, 0, 0) for the two different mesh densities, a mesh of 241 623 elements with the maximum edge size of 60 mm, and a mesh of 490 420 elements with the maximum edge size of 20 mm, from 80 s to 120 s

Slika 10: Temperatura in celotni raztezek v točki (0, 0, 0) za dve različni gostoti mreže: mreže z 241 623 elementi, maksimalna velikost roba 60 mm, in mrežo s 490 420 elementi, maksimalna velikost roba 20 mm, od 80 s do 120 s

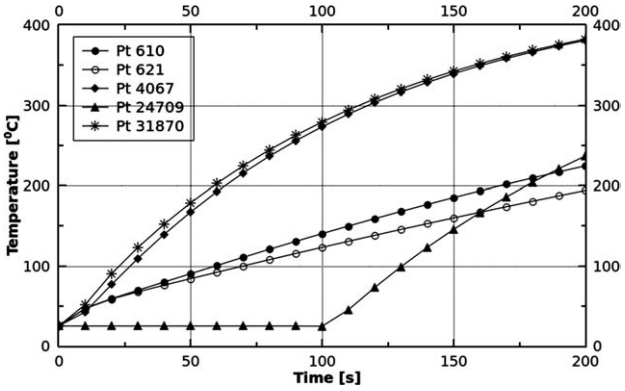

Figure 11: Temperature at different points of the skeleton, on and around the bottom-corner fitting, from the beginning of the simulation to 200 s, for the mesh of 490 420 elements

Slika 11: Temperatura v različnih točkah ogrodja na spodnjem vogalnem spoju in okrog njega od začetka simulacije do 200 s v primeru mreže s 490 420 elementi

Points 621 and 610 are on the bottom-corner fitting and their positions are equivalent to those of points 11 and 10, illustrated in **Figure 5**. As expected, the temperature of point 610 was higher than the temperature of point 621, as presented in the case of the corner fittings. Both temperatures were lower than the temperatures of the points on the bottom profiles.

The last presented point is at the front-corner post, just above the bottom-corner fitting. The thickness of the material of the front-corner post is 6 mm. This point starts to heat up 100 s after the above-presented points, but in the following 100 s it exceeds the temperature of the two points on the bottom-corner fitting.

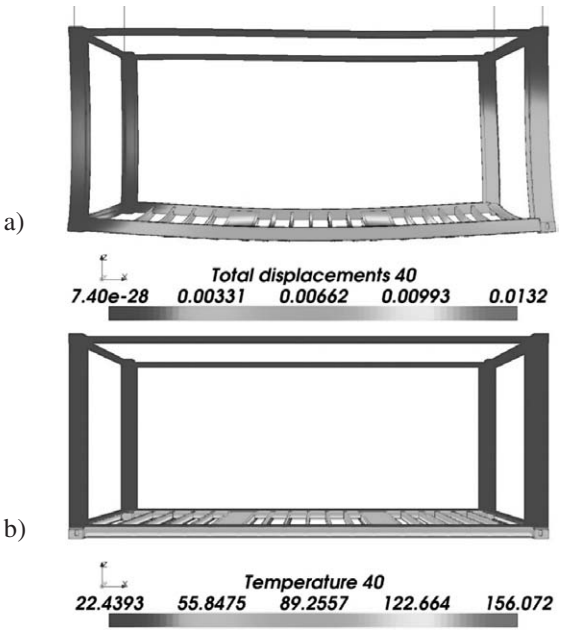

Figure 12: a) Total displacements (scale 20) and b) the temperature distribution at 40 s for the mesh of 490 420 elements

Slika 12: a) Skupni raztezek (skala 20) in b) razporeditev temperature pri 40 s za mrežo s 490 420 elementi

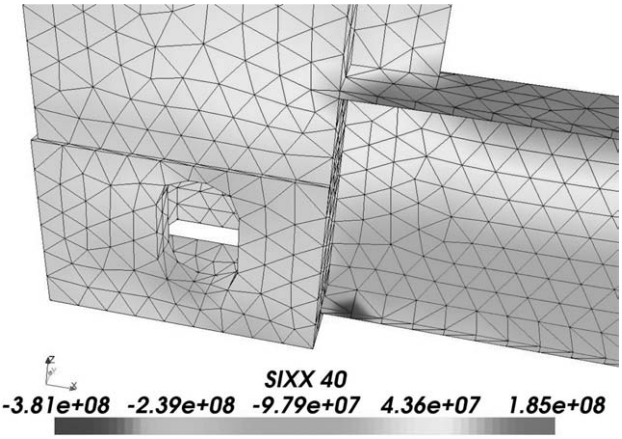

Figure 13: Maximum stress at the bottom side rail near the front-bottom-corner fitting at t = 40 s

Slika 13: Maksimalna napetost v spodnjem stranskem profilu blizu spodnjega sprednjega vogalnega spoja pri t = 40 s

The distributions for the finer mesh at 40 s are presented in **Figure 12**. While the minimum temperature for the coarse mesh at 50 s, presented in **Figure 9** (top right), was approximately 21 °C, for the finer mesh this value was around 22 °C at 40 s (**Figure 12b**). Also, the maximum value for the total displacements was almost 1 mm higher at 40 s for the finer mesh than at 50 s for the coarser mesh (**Figure 9** (top left)).

The maximal stresses at 40 s, illustrated in **Figure 13**, were located at the bottom of the bottom side rails near the front bottom-corner fittings. The bottom rail is planned to be made of 4.5 mm thick S420NL steel, and its maximum stress value is 381 MPa.

4 CONCLUSIONS

Three-dimensional linear thermal and nonlinear static analyses, of the top-corner fitting as a part of the container structure and of the entire skeleton as the container substructure, were performed to initiate the analysis of the distortion of a 20-ft ISO shipping container exposed to the temperature of a zinc hot-dip galvanizing bath. Numerical simulations were carried out using open-source CAE software: Salome-Meca, Netgen, and Code_Aster. The temperature was the only transient boundary condition. The temperature of the galvanizing bath, the velocity of immersion, and the thermomechanical properties of steel were kept constant during all the simulations. Tests were carried out within the limits of the very poor computer resources. However, satisfactory initial results were obtained and sufficient information was gathered to make a general image of the container-substructure behavior under the influence of the zinc hot-dip galvanizing-bath temperature.

Acknowledgements

The authors would like to acknowledge the financial support given under the EUREKA E! 5009 Galvacont project.

5 REFERENCES

[1] IGAG, INGAL Specifiers Manuel, Available: www.ingal.com.au/igsm.htm

[2] G. Livelli, T. Langill, Guidelines for Welding Galvanized Steel, PCI Journal, (**1998**), 40–48

[3] L. Mraz, J. Lesay, Problems with reliability and safety of hot dip galvanized steel structures, Soldagem and inspecao, 14 (**2009**) 2, 184–190

[4] H. Zhang, K. M. Moallemi, S. Kumar, Thermal Analysis of the Hot Dip-Coating Process, Journal of Heat Transfer, 115 (**1993**), 453–460

[5] M. Berković, S. Maksimović, A. Sedmak, Analysis of Welded Joints by Applying the Finite Element Method, Structural Integrity and Life, 4 (**2004**) 2, 75–83

[6] D. Veljić, M. Perović, A. Sedmak, M. Rakin, N. Bajić, B. Medjo, H. Dascau, Numerical Simulation of the Plunge Stage in Friction Stir Welding, Structural Integrity and Life, 11 (**2011**) 2, 131–134

[7] D. Veljić, M. Perović, A. Sedmak, M. Rakin, M. Trifunović, N. Bajić, D. Bajić, A Coupled Thermo-Mechanical Model of Friction Stir Welding, Thermal Science, 16 (**2012**) 2, 527–534

[8] M. Perović, D. Veljić, M. Rakin, N. Radović, A. Sedmak, N. Bajić, Friction-Stir Welding of High-Strength Aluminium Alloys and a Numerical Simulation of the Plunge Stage, Mater. Tehnol., 46 (**2012**) 3, 105–111

[9] W. J. Rudd, S. W. Wen, P. Langenberg, B. Donnay, A. Voelling, T. Pinger, M. Feldmann, J. Carpio, J. A. Casado, J. A. Alvarez, F. Gutierrez-Solana, Failure mechanisms during galvanising, Office for Official Publications of the European Communities, Luxembourg, 2008

[10] M. Feldmann, T. Pinger, D. Schäfer, R. Pope, G. Sedlacek, Hot-dip-zinc-coating of prefabricated structural steel components, Office for Official Publications of the European Communities, Luxembourg, 2010